

Solvent-Exposed Tails as Prestalk Transition States for Membrane Fusion at Low Hydration

Yuliya G. Smirnova,[†] Siewert-Jan Marrink,[‡] Reinhard Lipowsky,[†] and Volker Knecht*[†]

Max-Planck Institute of Colloids and Interfaces, Department of Theory and Bio-Systems, Research Campus Golm, D-14424 Potsdam, Germany, and Groningen Biomolecular Sciences and Biotechnology Institute & Zernike Institute for Advanced Materials, University of Groningen, Nijenborgh 4, 9747 AG Groningen, The Netherlands

Received November 27, 2009; E-mail: vknecht@mpikg.mpg.de

Abstract: Membrane fusion is a key step in intracellular trafficking and viral infection. The underlying molecular mechanism is poorly understood. We have used molecular dynamics simulations in conjunction with a coarse grained model to study early metastable and transition states during the fusion of two planar palmitoyl-oleoyl-phosphatidylcholine (POPC) bilayers separated by five waters per lipid in the *cis* leaflets at zero tension. This system mimics the contact area between two vesicles with large diameters compared to the membrane thickness at conditions where fusion may start in the core of the contact area. At elevated temperatures, the two proximal leaflets become connected via multiple lipid molecules and form a stalklike structure. At room temperature, this structure has a free energy of $3k_B T$ and is separated from the unconnected state by a significant free energy barrier of $20k_B T$. Stalk formation is initiated by the establishment of a localized hydrophobic contact between the bilayers. This contact is either formed by two partially splayed lipids or a single fully splayed one leading to the formation of a (metastable) splayed lipid bond intermediate. These findings indicate that, for low hydration, early membrane fusion kinetics is not determined by the stalk energy but by the energy of prestalk transition states involving solvent-exposed lipid tails.

Introduction

Membrane fusion is a key step during intracellular traffic, exocytosis or intracellular fusion (in particular synaptic transmission), recycling, protein trafficking, viral infection, fertilization, and drug delivery. Fusion is tightly controlled by proteins which bring selected membranes in close proximity, thus facilitating fusion. Fusion proteins denoted as soluble *N*-ethylmaleimide-sensitive factor attachment protein receptors (SNAREs) involved in intracellular traffic and exocytosis are believed to promote membrane fusion by bringing two membranes in close proximity.¹ Subsequent stages are considered to be primarily determined by the physics of lipids.

Before fusion may set in, two membranes have to come close to each other as shown in Figure 1a. The initial distance between the membranes would be 2–3 nm for lipid bilayer stacks at full hydration, as arising from a balance between short-range hydration and entropic repulsion versus long-range van der Waals attraction.² Dehydration of the intermembrane contact is likely involved in poly(ethylene glycol)-induced fusion of PC vesicles *in vitro*. *In vivo*, fusion proteins may bring membranes closer to each other by inducing local curvature³ or accumulation at the rim of an extended planar contact zone

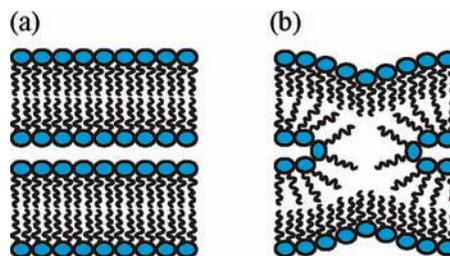


Figure 1. Early intermediates during fusion of lipid membranes: (a) two membranes in close proximity but separated (lamellar state); (b) stalk between the membranes.

between two membranes as observed for vacuole fusion in yeast.⁴ Such a process may involve partial dehydration as well.

In vitro experiments on protein-free systems⁵ led to the notion that the fusion of two such apposed lipid membranes is initiated by the formation of an intermembrane bridge formed by multiple lipid molecules later called a “stalk” and depicted in Figure 1b. The stalk will expand, such that the two distal leaflets get into contact, a state denoted as hemifused state. Stalks have been observed directly in experiments using X-ray scattering.^{6,7} It was found that, for low hydration and depending on the lipid

[†] Max-Planck Institute of Colloids and Interfaces.

[‡] University of Groningen.

(1) Sørensen, J. B. *Annu. Rev. Cell Dev. Biol.* **2009**, *25*, 513–537.

(2) Lipowsky, R.; Sackmann, E. In *Structure and Dynamics of Membranes*; Elsevier: Amsterdam, 1995; pp 521–602.

(3) Knecht, V.; Grubmüller, H. *Biophys. J.* **2003**, *84*, 1527–1547.

(4) Wang, L.; Seeley, E. S.; Wickner, W.; Merz, A. J. *Cell* **2002**, *108*, 357–369.

(5) Hui, S. W.; Stewart, T. P.; Boni, L. T.; Yeagle, P. L. *Science* **1981**, *212*, 921–923.

(6) Yang, L.; Huang, H. W. *Science* **2002**, *297*, 1877–1879.

(7) Yang, L.; Huang, H. W. *Biophys. J.* **2003**, *84*, 1808–1817.

composition, stalks between lipid lamellae are thermodynamically stable. This phase has also been observed in a molecular dynamics (MD) computer simulation study using a coarse grained (CG) model.⁸ Stable stalklike structures were also formed via self-assembly of hydrated lipids and fusion peptides in recent CG simulations, yielding a single bicontinuous cubic lipid phase corresponding to a phase of stable stalk–pore complexes.⁹ Likewise, stalklike structures have been observed in simulations of membrane fusion for partially dehydrated intermembrane contacts using CG^{10–16} or atomistic models.^{17–19}

MD simulations using a CG model with explicit solvent yielded $6k_B T$ for the free energy of stalks between small palmitoyl-oleoyl-phosphatidyl-ethanolamine (POPE) vesicles.¹³ From MD simulations using a generic solvent-free CG model, the free energy of a stalk between planar bilayers of amphiphiles was estimated as $15k_B T$.²⁰ Self-consistent field theory has also been used to estimate stalk energies which were found to be below $10k_B T$.²¹ In these latter calculations, lipids were described as amphiphilic diblock copolymers and water as a melt of hydrophilic homopolymers.

A continuum model for elastic energies of tilted and splayed lipids leads to a lower bound for the free energy of stalks between dipalmitoyl-oleoyl-phosphatidylcholine (DOPC) bilayers of $45k_B T$.²² A related model suggested that the free energy of a stalk arises from an interplay between (i) the elastic energy of lipid monolayers including a contribution of the saddle splay deformation and (ii) the energy of hydration repulsion between two apposing membranes.²³ Hence, at low hydration, the free energy of stalks may be negative,²³ explaining the existence of the stalk phase observed in experiment^{6,7} and simulation.⁸

For bilayers with lipid compositions typical for biological membranes at full hydration, estimates for stalk energies from the continuum models varied from 25 to $50k_B T$. The continuum models used in these studies rely on a series expansion of the energy density in powers of the membrane curvature and a truncation of this expansion after the two leading terms.²⁴ This truncation can be justified if there is a separation of length scales, that is, if the membrane curvature radii are large compared to the membrane thickness. Such a separation of length scales does not apply, in general, to stalklike structures since their curvature radii are often comparable to the membrane thickness.

It is often assumed that stalks, if thermodynamically unfavorable, provide the transition state for hemifusion, an assumption which is disputable. First, the stalks considered in the continuum theories are both axi- and top-down symmetric. Such a high symmetry is unlikely for a transient state. Second, two adhering membranes are presumably separated by hydration water bound at the lipid headgroups. Hence, in order to form a pointlike contact, water must be pushed to the side. Considering this in a continuum model, the barrier against stalk formation has been predicted to be well above the free energy of the stalk state itself.^{25,26}

Accordingly, the rate-limiting step during the fusion of two highly curved lipid vesicles in close proximity during molecular dynamics (MD) simulations using a coarse grained (CG) model was the merging of some head groups of one of the proximate leaflets with the opposing leaflet; the subsequent formation of a stalk and a hemifusion diaphragm appeared to be a downhill process.¹¹ A Markovian state model constructed from many short-time scale CG simulations using distributed computing suggested stalks during vesicle fusion to be even metastable.¹³ In fact, stalks may not necessarily form during membrane fusion. In recent dissipative particle dynamics (DPD) simulations of tension-induced fusion between lipid vesicles with a partially dehydrated intermembrane contact, stalks were observed during fusion at high but not at low tension.²⁷ In a related DPD simulation study, the critical step for the mixing of lipids between adhered bilayers under tension were interbilayer flips of single lipid tails.¹⁵ In the resulting splayed lipid bond state, the two bilayers were connected via a single lipid adopting a splayed conformation with one of its tails inserted in each of the two *cis* monolayers as proposed previously.²⁸

To model early fusion events in the core of the contact zone of vesicles with diameters large compared to the membrane thickness at zero tension, two planar phospholipid bilayers apposed are considered in this paper. MD simulations in conjunction with a CG model have been used to study respective early fusion intermediates. We use the term “intermediates” for both transition and metastable states. The system studied consisted of palmitoyl-oleoyl-phosphatidylcholine (POPC) bilayers separated by five waters per lipid in the *cis* leaflets at zero tension. POPC is abundant in biological membranes and dehydration of PC bilayers may induce their fusion.^{29,30}

In our simulations, the two bilayers remained separated for tens of microseconds. Formation of early fusion intermediates on a submicrosecond time scale was induced by simulations at elevated temperature or by applying a harmonic potential to a selected lipid molecule. Fixing one of the tails of this lipid molecule between the bilayers induced the formation of a stalk on a nanosecond time scale. The free energy of the stalk is found to be lower than that of various prestalk intermediates identified as new transition states. Thus, for fusion starting from a partially dehydrated intermembrane contact, the stalk itself is not a transition state but either metastable or on the downhill slope of the fusion process.

- (8) Marrink, S. J.; Mark, A. E. *Biophys. J.* **2004**, *87*, 3894–3900.
 (9) Fuhrmans, M.; Knecht, V.; Marrink, S. J. *J. Am. Chem. Soc.* **2009**, *131*, 9166–9167.
 (10) Noguchi, H.; Takasu, M. *J. Chem. Phys.* **2001**, *115*, 9547–9551.
 (11) Marrink, S. J.; Mark, A. E. *J. Am. Chem. Soc.* **2003**, *125*, 11144–11145.
 (12) Stevens, M. J.; Hoh, J. H.; Woolf, T. B. *Phys. Rev. Lett.* **2003**, *91*, 188102(4).
 (13) Kason, P. M.; Kelly, N. W.; Singhal, N.; Vrljic, M.; Brunger, A. T.; Pande, V. S. *Proc. Natl. Acad. Sci. U.S.A.* **2006**, *103*, 11916–11921.
 (14) Shillcock, J.; Lipowsky, R. *Nat. Mater.* **2005**, *4*, 225–228.
 (15) Grafmüller, A.; Shillcock, J.; Lipowsky, R. *Phys. Rev. Lett.* **2007**, *2007*, 218101(4).
 (16) Smeijers, A. F.; Markvoort, A. J.; Pieterse, K.; Hilbers, P. A. J. *J. Phys. Chem. B* **2006**, *110*, 13212–13219.
 (17) Marrink, S. J.; Tieleman, D. P. *Biophys. J.* **2002**, *83*, 2386–2392.
 (18) Knecht, V.; Mark, A.; Marrink, S. J. *J. Am. Chem. Soc.* **2006**, *128*, 2030–2034.
 (19) Knecht, V.; Marrink, S. J. *Biophys. J.* **2007**, *92*, 4254–4261.
 (20) Norizoe, Y.; Daoulas, K. C.; Müller, M. *Faraday Discuss.* **2010**, *144*, 369–391.
 (21) Katsov, K.; Müller, M.; Schick, M. *Biophys. J.* **2004**, *87*, 3277–3290.
 (22) Kozlovsky, Y.; Kozlov, M. M. *Biophys. J.* **2002**, *82*, 882–895.
 (23) Kozlovsky, Y.; Efrat, A.; Siegel, D. A.; Kozlov, M. M. *Biophys. J.* **2004**, *87*, 2508–2521.
 (24) Seifert, U.; Lipowsky, R. In *Structure and Dynamics of Membranes*; Elsevier: New York, 2005; p 403.

- (25) Kuzmin, P. I.; Zimmerberg, J.; Chizmadzhev, Y. A.; Cohen, F. S. *Proc. Natl. Acad. Sci. U.S.A.* **2001**, *98*, 7235–7240.
 (26) Shillcock, J.; Lipowsky, R. *J. Phys. Cond. Matter* **2006**, *18*, S1191–S1219.
 (27) Gao, L.; Lipowsky, R.; Shillcock, J. *Soft Matter* **2008**, *4*, 1208–1214.
 (28) Kinnunen, P. K. J. *Chem. Phys. Lipids* **1992**, *63*, 251–258.
 (29) Boni, L. T.; Stewart, T. P.; Alderfer, J. L.; Hui, S. W. *J. Membr. Biol.* **1981**, *62*, 71–77.
 (30) Chernomordick, L. V.; Kozlov, M. M.; Melikyan, G. B.; Abidor, I. G.; Markin, V. S.; Chizmadzhev, Y. A. *Biochim. Biophys. Acta* **1985**, *812*, 643–655.

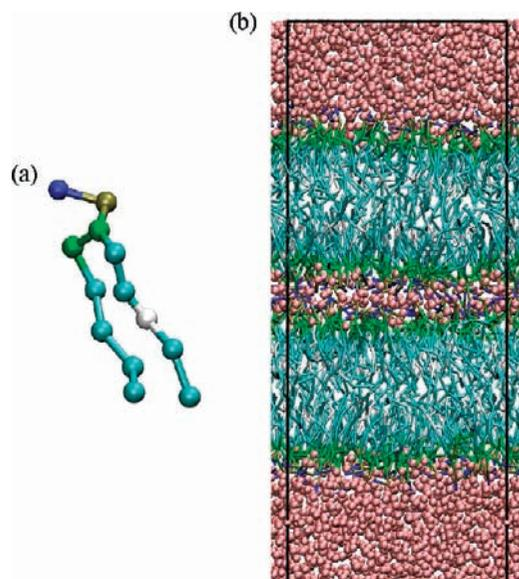


Figure 2. Simulated system: (a) single POPC molecule; (b) simulation box with two POPC bilayers and two water layers. Colors distinguish between choline (blue), phosphate (tan), glycerol (green), the saturated alkyl chains (cyan), and the unsaturated bond (white). Water beads are shown as pink spheres.

Table 1. Equilibrium Simulations of System^a

$t = 0$	N_{sim}	Δt	T (K)
lamellar	1	40 μs	300
splayed lipid bond	15	400 ns	300
stalk	15	16 μs	300
lamellar	10	2.4 μs	380

^a The initial state, $t = 0$, the number of simulations, N_{sim} , the effective time scale per simulation, Δt , and the temperature, T , are given. Multiple simulations of the same state were started from different initial configurations taken from a simulation at equilibrium (lamellar or stalk state) or with a harmonic potential subjected to a selected lipid (splayed lipid bond).

Results

Stalklike Lipid Bridges between Bilayers. To understand the stability of early membrane fusion intermediates, the system comprising two tension-free POPC bilayers as in Figure 2 was studied at equilibrium using different initial states; see Table 1. The pressure lateral and normal to the bilayers was separately coupled to 1 bar corresponding to zero tension, and the temperature chosen was 300 K. The system included two water layers of different thicknesses. In principle, water can diffuse through the bilayers, and a net flux from the high to the low hydration water layer would lead to equal water content in both layers on long time scales. However, this process is slow and can be neglected on the time scales considered here. When the bilayers were initially separated as in Figure 3a, they remained so during a 40 μs simulation. In contrast, when the unsaturated tail of a lipid molecule was fixed in the center of the water layer, a connection between the bilayers consisting of multiple lipids formed on a nanosecond time scale. The width of this connection grew until an equilibrium size as in Figure 3d was reached after ~ 20 ns. The lipid connection with this equilibrium size shall be denoted as stalk. This state was stable during a 16 μs simulation even in the absence of an umbrella potential.

Properties of Stalklike Structures. As schematically shown in Figure 1b and indicated from the highlighted lipid in Figure 3d, the lipids in the stalk tilt away from the center of the stalk.

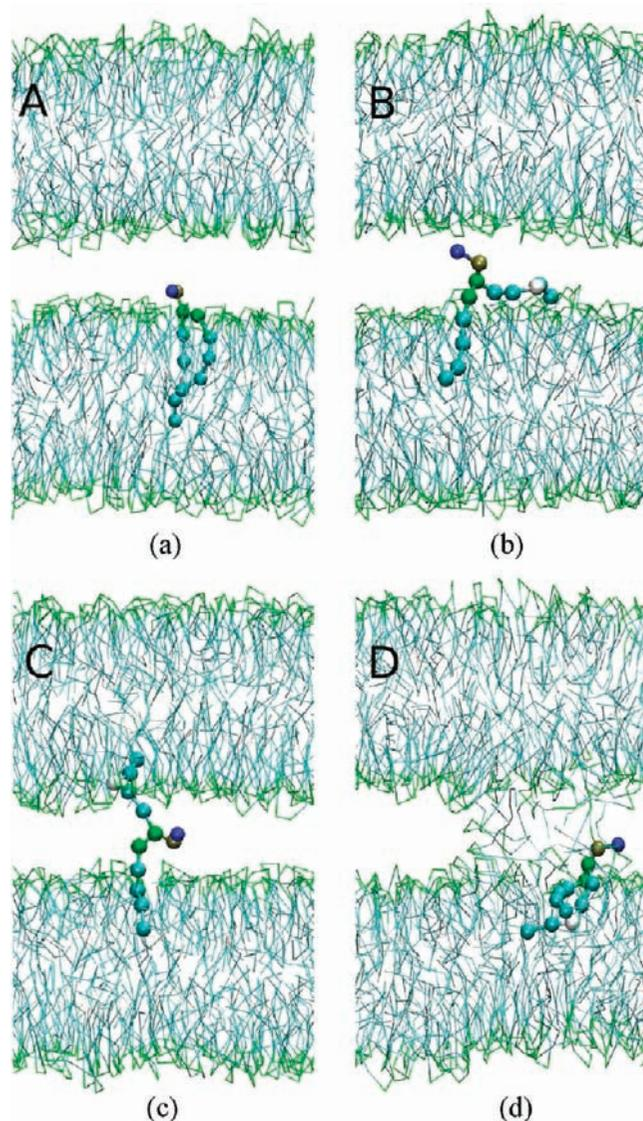


Figure 3. Representative configurations of early states during membrane fusion. (a) lamellar state; (b) “L” state; (c) splayed lipid bond; (d) stalk. The a,c,d states are metastable, while b corresponds to a plateau region. The representation is similar to that chosen in Figure 2. The lipid to which a harmonic potential is applied is depicted as bonds and beads. Water beads and choline and phosphate groups of the remaining lipids are not shown.

The configuration depicted in Figure 3d, though, differs from the schematic representation in Figure 1b in two aspects. First, the lipid packing in the stalk region is rather disordered. Second, the top-down symmetry is broken in that the lower but not the upper distal leaflet exhibits a dimple. Figure 4a showing a time-averaged tail density for the stalk, though, suggests that the top-down symmetry is regained in the average. The distribution of the tails in the hydrophobic core of the stalk is uniform except the well-known density dip between the two leaflets of each bilayer. This indicates that voids, an energetic issue in early stalk models, are prevented by suitable lipid packing, as suggested from stalk structures proposed in analytical studies.^{22,25,31}

The respective headgroup density shown in Figure 4b reveals that headgroups surround the stalk but are absent in its center. Thus, the stalk observed here exhibits a purely hydrophobic core as predicted from continuum models and previous MD

(31) Markin, V. S.; Albanesi, J. P. *Biophys. J.* **2002**, *82*, 693–712.

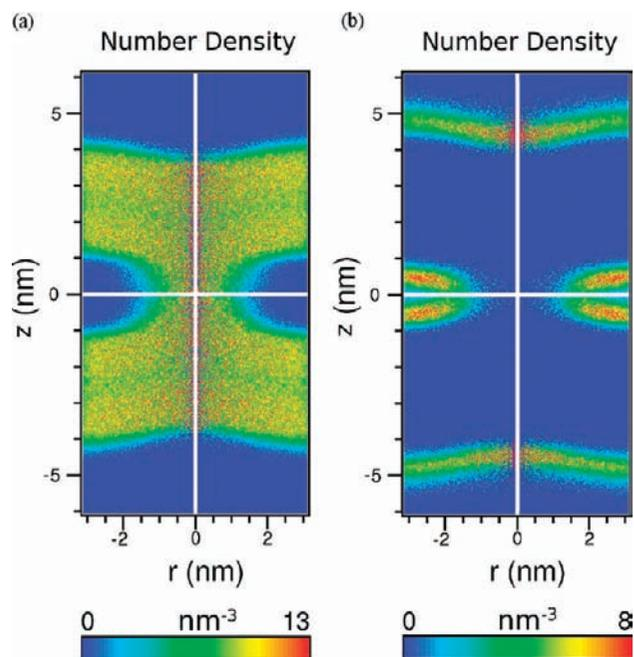


Figure 4. Distribution of (a) tails and (b) head groups (choline and phosphate) in a stalk as a function of the position z along an axis through the center of the stalk and the distance r from the axis averaged over 80 ns. The grid spacing is 0.02 nm.

simulations.^{11,16–19} This is in contrast to more disordered interbilayer bridges with lipid headgroups trapped in their interior observed in previous DPD simulations of tension-induced fusion.³²

The number of lipids in the stalk, N_L , is estimated from $N_L = V_S/V_L$ where V_S or V_L denote the volume of the hydrophobic portion of a stalk and a lipid, respectively. The tail portion of the lipid is considered a cylinder with a cross-section area equal to the area per lipid in a bilayer, a_L , and a height h_L . Likewise, a stalk is considered as a cylinder with radius r_S and height h_S . A fit to the distribution of tails in Figure 4a yields $h_S = 2$ nm, $r_S = 1$ nm, and $h_L = 1.4$ nm. Analysis of a trajectory of the lamellar state leads to $a_L = 0.6$ nm². Hence, $N_L = \pi r_S^2 h_S / a_L h_L \approx 7.5$.

Due to the water confined in the thin layer separating the bilayers for the boundary conditions chosen, the stalk is stabilized against later fusion intermediates in our system. We note, though, that these downstream fusion stages are beyond the scope of this work. Most importantly, the stability of the stalk and the lamellar state indicates that the two states are separated by a high free energy barrier. Thus, the stalk is not a transition state but either metastable or on the downhill slope of the fusion process.

In order to surmount this energy barrier to identify possible transition pathways, ten 2.4 μ s simulations were started from the lamellar state at an elevated temperature of 380 K. In these simulations, stalks formed spontaneously, either directly or (in six out of ten simulations) via a splayed lipid bond shown in Figure 3c. A preformed splayed lipid bond at room temperature showed an average lifetime of 100 ns before transforming back to the lamellar or the stalk state in a series of simulations. Here, the lamellar and the stalk state were adopted seven or eight

times, respectively, that is, within the statistical error with equal probability.

Free Energy Landscape of Stalk Formation. Figure 5a shows a one-dimensional projection of the free energy landscape underlying early fusion stages at 300 K. This projection is the potential of mean force (PMF) along the displacement z_T of the center-of-mass of the unsaturated tail of a selected lipid molecule from the center of the water layer along the bilayer normal. The PMF profile was determined by subjecting z_T to a harmonic potential centered at different positions in a set of simulations (umbrella sampling). For comparison, the distribution of water, lipid head groups, and tails as well as the double bonds of the lipid tails normal to the bilayer (z axis) in the absence of the umbrella potential are shown in Figure 6. Here, the origin of the z axis is chosen to be in the center of the water layer to enable direct comparison with the reaction coordinate z_T . Figure 5a shows the PMF along z_T , $G_1(z_T)$, from umbrella sampling using either 8 or 16 μ s of simulation time per umbrella window. As expected, the minimum of the PMF at $z_T = -1.8$ nm is close to the maximum in the distribution of the lipid double bonds at $z = \pm 1.9$ nm. The minimum of the PMF along z_T does not precisely coincide with the maximum in the distribution of the lipid double bonds because the position of the double bond does not exactly correspond to the center-of-mass of the unsaturated tail. The PMF rises steeply upon moving the lipid tail toward the center of the bilayer and somewhat less steeply upon moving the tail toward the water region until a plateau region at about -0.6 nm is reached. Increasing the time scale for the umbrella windows decreases the value of the PMF in the plateau region. The value of the PMF at finite time scales thus represents an upper bound for the respective real value.

To obtain more detailed information about the free energy landscape, a second reaction coordinate was considered. This coordinate was chosen as the minimal distance between the hydrophobic cores of the bilayers considering all lipid except the one subjected to the umbrella potential, u . For a given configuration, u is defined via

$$u \equiv \min_{(i,j), i \in A, j \in B} d(i,j) \quad (1)$$

Here, set A consists of all tail beads in the upper bilayer, set B comprises all tail beads in the lower bilayer except the tails of the lipid restrained by the external potential, and $d(i,j)$ denotes the distance between bead i and bead j . The relation between u and the distance between the centers of mass of the bilayers in z direction is discussed in the Supporting Information. The two-dimensional PMF profiles $G_2(z_T, u)$ from $G_1(z_T)$ and the histograms $H_{z_T}(u)$ for given z_T windows are shown in Figure 5b,c. Note that only z_T but not u was imposed in the simulations. That is, $H_{z_T}(u)$ was obtained from the spontaneous fluctuations in u for given z_T . The two figures correspond to simulation times of 8 or 16 μ s, respectively, per umbrella window. Here, the global minimum A characterized by -2.6 nm $< z_T < -0.3$ nm and 0.8 nm $< u < 1.9$ nm corresponds to the lamellar state shown in Figure 3a. A plateau region B for -0.25 nm $< z_T < 0.1$ nm and 1.2 nm $< u < 1.6$ nm corresponds to a state in which the unsaturated tail resides at the boundary between the tail and headgroup region and orients parallel to the bilayer such that the lipid forms an “L state” as shown in Figure 3b. The local minimum C at 0.4 nm $< z_T < 0.7$ nm and 0.9 nm $< u < 1.6$ nm represents the splayed lipid bond shown in Figure 3c. States with 0.45 nm $< u < 0.7$ nm correspond to the stalk intermediate.

(32) Grafmüller, A.; Shillcock, J.; Lipowsky, R. *Biophys. J.* **2009**, *96*, 2658–2675.

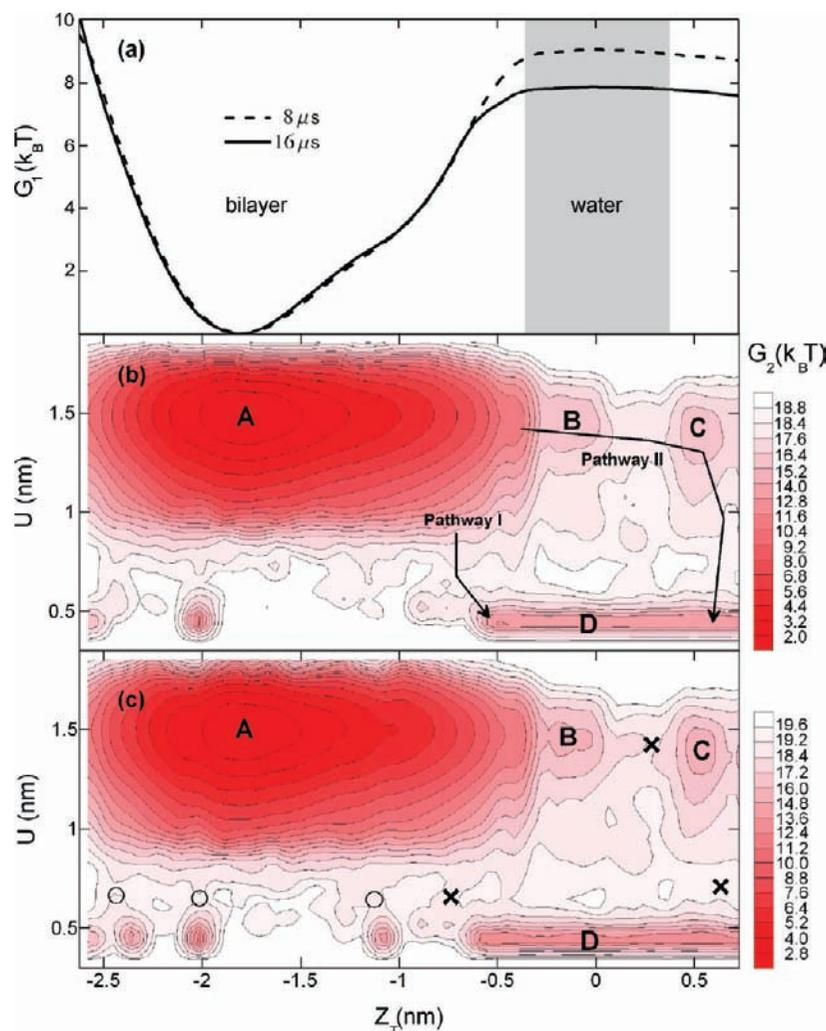


Figure 5. One- and two-dimensional projections of the free energy landscape underlying early membrane fusion intermediates in terms of potential of mean force (PMF) profiles along preselected reaction coordinates. (a) 1D PMF profile along the displacement z_T of the center-of-mass of the unsaturated lipid tail of a selected lipid from the center of the water layer normal to the bilayer. The PMF profile was obtained from a set of simulations in which z_T was imposed at different values (umbrella sampling). (b,c) 2D PMF landscape for z_T and the minimum distance u between centers-of-mass of the hydrophobic cores of the bilayers except the selected lipid as a second reaction coordinate. The 2D PMF is determined from the 1D PMF profile and the spontaneous fluctuations of u at given values of z_T via eq 2. The bin width for z_T or u is 0.005 or 0.003 nm, respectively, and low-pass Gaussian filtering is used. Consider that $1k_B T = 2.5$ kJ/mol for $T = 300$ K and the error is $1.5k_B T$. The PMF is color-coded, dark colors corresponding to low energies as indicated in the legend. Note that all simulations were started in the region A; white regions indicate regions of high energy or kinetically inaccessible on the microsecond time scale of the simulations. In a state with $u = 0.45$ nm, the hydrophobic cores of the bilayers (not counting the lipid related to z_T) form a *local* contact with no water in between; the total number of water molecules between the bilayers is kept constant. The minima correspond to the lamellar state (A), the splayed lipid bond (C), and the stalk (D). The plateau region B corresponds to the “L” state. Transition states are marked with crosses or circles. The transition states marked with circles correspond to the transition state for the leftmost cross (except for the fact that not the lipid for which z_T is shown participates in the first hydrophobic interbilayer contact but two other lipids). Representative configurations of these states are shown in Figure 3 or Figure 7, respectively.

States with $u < 0.45$ nm do not occur as they would correspond to van der Waals overlaps.

We note that the simulations were started from the global minimum and regions corresponding to the stalk state were sampled due to spontaneous transitions in u for given z_T . The stalk state exhibits an extended minimum for -0.7 nm $< z_T < 0.73$ nm. In this region, stalks form on a nanosecond time scale if an umbrella potential is present. In addition, the stalk shows also four localized minima for $z_T < -0.7$ nm. At these positions, the stalks form on a microsecond time scale and the number of these minima increases when the time scale for the umbrella windows is increased from 8 to 16 μ s. The energy barriers to be overcome here are lower for $z_T \sim 0$ than otherwise, thus, stalks form earlier for $z_T \sim 0$ than away from this point. The localized minima indicate the stochastic nature of the stalk

formation process. At infinitely long time scales we expect the region corresponding to the stalk to form a single connected minimum. At finite time scales, sampling is complete for the lamellar but not for the stalk region, so the estimate for the free energy of the stalk relative to the lamellar state obtained will be an upper bound.

Note that the formation of stalks in the presence of an umbrella potential does not contradict the observation above that no stalk is formed on a time scale of 40 μ s at equilibrium. This is because the presence of the umbrella potential likely alters the kinetics of the system. Although fixing a lipid tail close to its equilibrium position may barely affect the energy barrier ΔG^\ddagger against stalk formation, it likely decreases the relaxation times for neighboring lipids and thereby increases the attempt frequency r_0 . The stalk formation rate r given by r

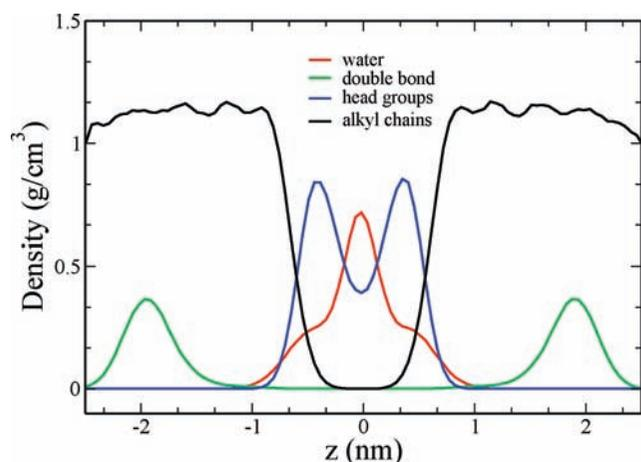


Figure 6. Distribution of water, double bonds, head groups, and alkyl chains normal to the bilayer at equilibrium averaged over 640 ns. The bin width is 0.3 nm.

$= r_0 \exp(-\Delta G^\ddagger/k_B T)$ with k_B and T denoting Boltzmann's constant and the temperature, respectively, will be increased accordingly.

Partial partition functions for the lamellar, the "L" state, the splayed lipid bond, and the stalk state from $G_z(z_T, u)$ and Boltzmann inversion yield free energies relative to the lamellar state. The free energy of the L state and the splayed lipid bond is estimated as $14k_B T$ and the free energy of the stalk as at most $3k_B T$ (see eq 4). The free energy barriers between the splayed lipid bond and the lamellar or the stalk state, respectively, were similar and about $4k_B T$. Again, the similarity of the energy barriers is in agreement with our observations that a preformed splayed lipid bond transforms into a stalk or the lamellar state with about equal probability at room temperature.

The free energy landscape in Figure 5 suggests that, at equilibrium, a stalk forms directly (pathway I) or via the L state and the splayed lipid bond (pathway II). Visual inspection of the trajectories show that stalk formation at $z_T < -0.3$ nm proceeds as in pathway I except for the fact that not the lipid for which z_T is shown but two other lipids participate in the initial hydrophobic contact between the bilayers; hence, this pathway is equivalent to pathway I. Significant energy barriers characterize the transitions (i) from the lamellar state directly

to the stalk in pathway I as well as (ii) from the lamellar state to the splayed lipid bond and (iii) the splayed lipid bond to the stalk state in pathway II. The free energy barriers for the transitions from the lamellar state to the stalk or the splayed lipid bond from the PMF are $\sim 18-20k_B T$. As these energy barriers correspond to the main barriers of the two pathways, their similarity is in agreement with our observations that stalk formation at elevated temperatures occurred via both pathways with about equal probability. The rate of stalk formation estimated from the energy barrier and the fluctuations of lipid tails normal to the bilayer in the lamellar state via eq 5 is 0.03 s^{-1} times the number of lipids in the contact area.

Identification of Transition States. A representative configuration for the transition state I between the lamellar state and the stalk is shown in Figure 7a. Here, two lipids in close vicinity, one from each of the two proximate leaflets, simultaneously adopt a partially splayed lipid conformation; each of the lipids stretches one of its tails toward the opposing leaflet such that a hydrophobic contact between the bilayers is established. The transition state II between the lamellar state and the splayed lipid bond is depicted in Figure 7b. Here, a single lipid molecule adopts a splayed conformation with one of its tails still inserted in the original leaflet while the second one crosses the gap between the hydrophobic cores of the two bilayers, just touching the distal hydrophobic core. Finally, the transition state between the splayed lipid bond and the stalk state is shown in Figure 7c. It corresponds to a splayed lipid bond where, in addition, tails in the vicinity of the splayed lipid bond approach the opposing leaflet.

In order to follow the dynamics along pathway I, we started simulations from transition state I in the absence of an umbrella potential. In four out of 11 simulations, the lamellar state formed within 4 ns, whereas a stalk was formed within 24 ns in seven simulations. Figure 8 shows the time evolution of the number of hydrophobic contacts between the bilayers. Here, two CG beads are considered in contact if their distance is below 0.6 nm. In the plot, fluctuations with frequencies of 0.1 ns^{-1} or higher are filtered out. For $t = 0$ corresponding to the transition state, 15 contacts are formed. The number of contacts increases linearly with time until a plateau with 105 contacts is reached after 25 ns. After 30 ns, the number of contacts starts to increase again. Respective configurations are shown in Figure 9. Initially

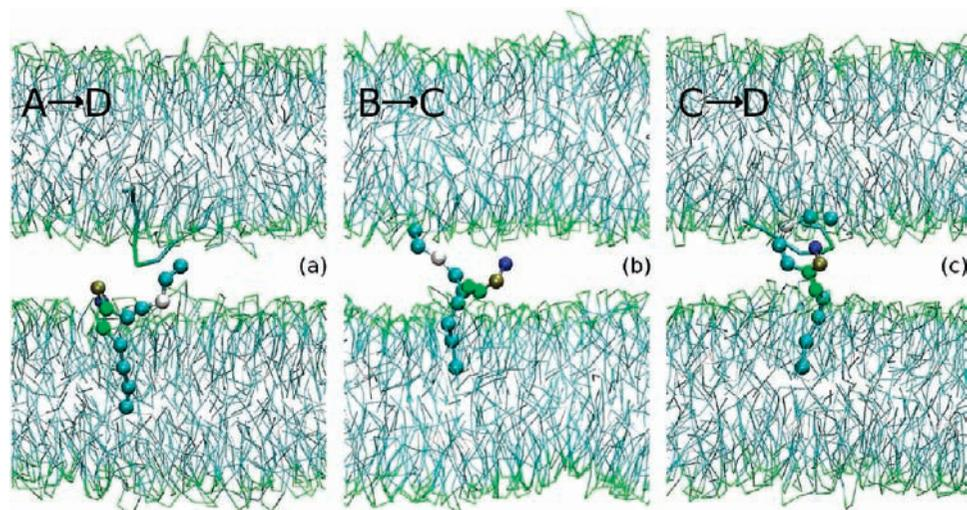


Figure 7. Representative configurations of prestalk transition states for membrane fusion. Transition states between the lamellar and (a) the stalk or (b) the splayed lipid bond and (c) between the splayed lipid bond and the stalk are shown. The representation is similar to that chosen in Figure 3.

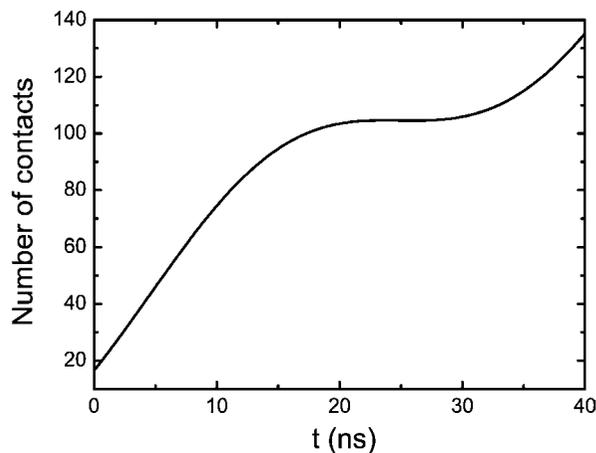


Figure 8. Time evolution of the number of hydrophobic contacts between two bilayers. Fourier components with frequencies above 0.1 ns^{-1} are filtered out using a fast Fourier transformation filter.

only two lipids, one from each of the proximal leaflets, participate in the lipid connection as depicted in Figure 9a. Subsequently, other lipids join this connection (Figure 9b–f), until a steady state reflecting the plateau region in Figure 8 is reached (Figure 9g). The configurations adopted during this process are quite disordered with L or splayed lipid conformations forming transiently as shown in Figure 9c,d. After the stalk has expanded to steady-state size, lipids diffuse through the stalk, thus being exchanged between the proximal leaflets of the two bilayers as depicted in Figure 9h and reflecting the second increase in the number of contacts in Figure 8. Lipid mixing between vesicles visualized by fluorescence quenching assays is often used to monitor vesicle fusion experimentally.^{33,34}

Discussion

The free energy of early membrane fusion intermediates is expected to strongly depend on the hydration level, the lipid type, and the temperature. We have used MD simulations in conjunction with a CG model to study early steps during the

fusion of two planar tension-less POPC bilayers separated by five waters per lipid in the proximate leaflets. Partial dehydration of the intermembrane contact may mimic conditions for polyethylene glycol-induced fusion of PC vesicles in vitro or protein-induced fusion in vivo where fusion proteins may accumulate at the rim of an extended planar contact zone between a vesicle and the target membrane.⁴ As shown in Figure 10, our results suggest that planar PC bilayers at low hydration do fuse via a stalk intermediate with a free energy of at most $3k_B T$. The low free energy for the stalklike structure is consistent with the results of earlier studies based on continuum models for the elastic energy of lipid monolayers including a contribution of the saddle splay deformation and the energy of hydration repulsion between two apposing membranes. It was found in these studies that, for a partially dehydrated intermembrane contact, stalk energies can be arbitrarily small and even negative.²³

A prestalk intermediate on one of the fusion pathways is a state in which a lipid adopts a conformation where its tail resides in the headgroup region but is not inserted into the water layer yet such that the molecule adopts an L shape. This state denoted as L state corresponds to a plateau region and exhibits a free energy of $14k_B T$. Lipids in the L state have also been observed in previous CG simulations of small vesicles¹⁶ and atomistic MD simulations of planar bilayers. For the planar bilayers, the probability of the L state was found to increase with decreasing hydration between the bilayers.³⁵

For a partially dehydrated intermembrane contact as considered here, the main barrier does not arise from a stalklike but a prestalk structure. The rate-limiting step for stalk formation between two bilayers is the establishment of a hydrophobic contact between the bilayers. The contact may be established via two possible pathways both involving solvent-exposed lipid tails and energy barriers of $20k_B T$. Either two lipids, one from each of the opposing leaflets in close proximity, simultaneously adopt a partially splayed lipid conformation such that their tails meet in the water and headgroup region between separating the hydrophobic cores of the bilayers (pathway I). Alternatively, a

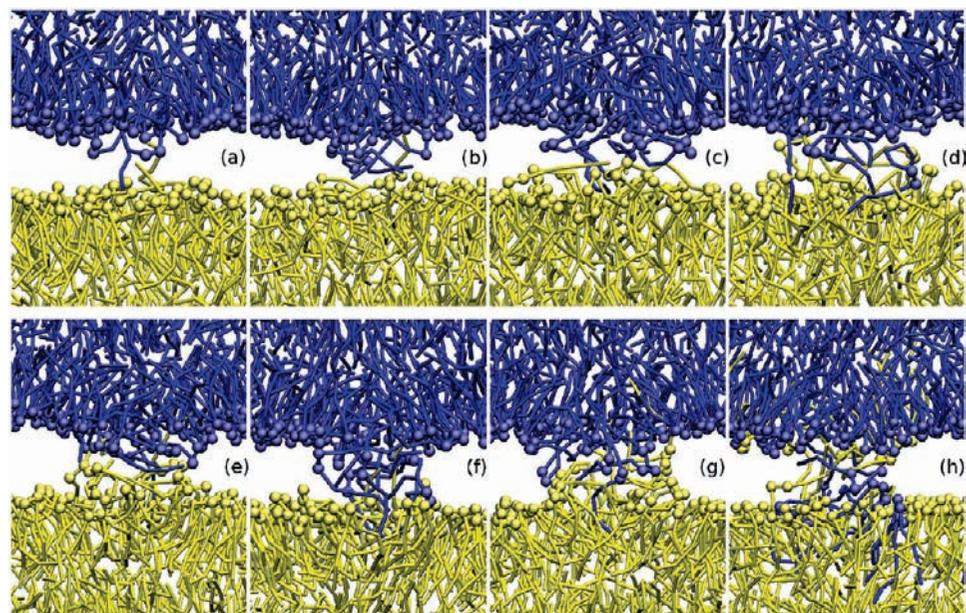


Figure 9. Configurations along the stalk formation pathway I (from A directly to D as shown in Figure 5) showing the transition state at $t = 0$ (a) and configurations after 4 ns (b), 8 ns (c), 12 ns (d), 16 ns (e), 20 ns (f), 40 ns (g), and 400 ns of simulation (h). Colors (blue and yellow) distinguish between the leaflets lipids resided initially. Tails are shown as sticks, and the glycerol backbone is depicted as spheres.

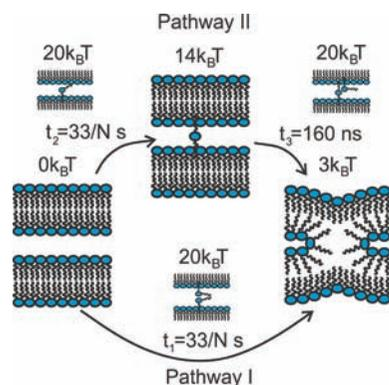


Figure 10. Early membrane fusion energetics and kinetics for two POPC bilayers separated by five waters per lipid. Metastable and transition states are shown schematically; for transition states, only the opposing leaflets are depicted. Metastable states consist of the lamellar state (left), the splayed lipid bond (middle), and the stalk (right). Each state of the systems is characterized by its excess free energy relative to the free energy of the lamellar state. Transition times from the splayed lipid bond to the lamellar or the stalk state were determined from spontaneous transitions observed in simulations. Transition times for interbilayer flips leading to the splayed lipid bond or direct transitions from the lamellar to the stalk state were estimated from the respective free energy barrier and the fluctuations of lipids normal to the bilayer using eq 5. Note that the transition times t_1 and t_2 depend on the number of lipids in the proximate leaflets, N .

single lipid might cross the whole gap between the hydrophobic cores of the bilayers, just touching the distal hydrophobic core. This transition state denoted as splayed lipid prebond is obligatory for formation of a splayed lipid bond which is metastable. The splayed lipid bond will either disappear or lead to the formation of a stalk (pathway II) with transition times of ~ 280 ns or ~ 160 ns, respectively.

A splayed lipid bond between the membranes studied here disappears as soon as other lipids join the intermembrane connection, resulting in a lipidic bridge with a pure hydrophobic core as observed in previous MD studies.^{11,16–19} Aggregated splayed lipid bonds hypothesized by Kinnunen²⁸ or lipid headgroups trapped in the core of the intermembrane connection as in DPD simulations tension-induced fusion¹⁵ were not observed. The main prestalk energy barriers may be used to estimate transition rates according to eq 5, yielding 0.03 per second times the number of lipids in the contact area. For a contact area similar to that investigated here, a transition time of ~ 260 ms is obtained. Here we assume that interbilayer flips are mainly performed by the unsaturated tail of the lipids as suggested previously.²⁸ That is, we neglect flips of the saturated tails in our rate calculations.

Our estimate for the free energy barrier against interbilayer flips between planar PC membranes is twice as large as that from previous DPD simulations.¹⁵ The difference to the results from the DPD study might reflect a difference in the hydration. Simulations using a coarse grain model probing the rates for stalk formation in bilayer stacks at different hydration levels suggest the respective energy barrier to be sensitive to the hydration level.⁸ For the DPD study, the hydration level was low similar to our study but not well-defined due to the lower resolution of the model.³⁶

We note that typical CG simulations of vesicle fusion have focused on vesicles with diameters in the range 15–17 nm. Here, curvature effects will be exaggerated compared to native trafficking vesicles having diameters between 40 and 80 nm.³⁷ Our study of planar bilayers modeling vesicles with large diameters compared to the membrane thickness complement the CG studies of vesicles in terms of the estimation of the barrier against stalk formation. A lower bound for the prestalk barrier is obtained from studies of small vesicles^{13,16,38} while our work gives an upper bound.

Our study provides a detailed view of prestalk membrane fusion kinetics and energetics. In particular, it shows that, for a partially dehydrated intermembrane contact, early membrane fusion kinetics is not determined by the stalk energy as often assumed but the energy of prestalk transition states involving solvent-exposed lipid tails.

Conclusions

We have used MD simulations in conjunction with a coarse grain model to investigate early events during membrane fusion and free energies of associated intermediates. Unlike assumed in most continuum models, for a partially dehydrated intermembrane contact, a stalk is separated from the lamellar state by a significant energy barrier. For such conditions, stalk formation is initiated by the establishment of a localized hydrophobic contact between the bilayers; this contact is either formed by two partially splayed lipids or a single fully splayed one leading to the formation of a (metastable) splayed lipid bond intermediate. This work opens the perspective to study in detail how early membrane fusion kinetics and energetics are affected by the physicochemical conditions (lipid composition, hydration, presence of fusion peptides).

Methods

The system considered in this work was studied under periodic boundary conditions using the MARTINI coarse grained (CG) model³⁹ as shown in Figure 2. It consisted of two POPC bilayers with 256 lipids and 2080 water beads with an initial box size $6.1 \times 6.4 \times 15.4$ nm³ at constant temperature and pressure. The pressure lateral and normal to the bilayers were separately coupled to 1 bar corresponding to zero tension. The system contained two separate water layers, one corresponding to five and the other to 60 water molecules per lipid in contact with the respective water layer. Details of the simulation protocol are given in the Supporting Information.

In order to identify possible stalk formation pathways, simulations starting from the lamellar state at an elevated temperature of 380 K as indicated in Table 1 were performed. All other simulations were conducted at room temperature (300 K). In particular, the stability of various intermediates was studied by performing simulations at equilibrium choosing different initial states as also summarized in Table 1.

In order to study the energetics of early fusion intermediates, a one- (1D) and a two-dimensional (2D) projection of the underlying free energy landscape were determined based on the potential of mean force along prechosen reaction coordinates.⁴⁰ For the 1D projection, the reaction coordinate was the displacement of the center-of-mass of the unsaturated tail of a selected lipid molecule from the center of the water layer normal to the bilayer. The value

(33) Murata, M.; Sugahara, Y.; Takahashi, S.; Ohnishi, S. *J. Biochem.* **1987**, *102*, 957–962.

(34) Zellmer, S.; Cevc, G.; Risse, P. *Biochim. Biophys. Acta* **1994**, *1196*, 101–113.

(35) Ohta-Iino, S.; Pasenkiewicz-Gierula, M.; Takaoka, Y.; Miyagawa, H.; Kitamura, K. *Biophys. J.* **2001**, *81*, 217–224.

(36) Grafmüller, A. Private communication.

(37) Takamori, S.; et al. *Cell* **2006**, *127*, 831–846.

(38) Kasson, P. M.; Pande, V. S. *PLoS Comput. Biol.* **2007**, *3*, 2228–2238.

(39) Marrink, S. J.; Risselada, H. J.; Yefimov, S.; Tieleman, D. P.; de Vries, A. H. *J. Phys. Chem. B* **2007**, *111*, 7812–7824.

(40) Torrie, G.; Valleau, J. *J. Comput. Phys.* **1977**, *23*, 187–199.

of z_T was restrained at 52 different equidistant values or “windows” in the interval from -2.6 to $+0.73$ nm using a harmonic potential with a force constant of $500 \text{ kJ mol}^{-1} \text{ nm}^{-2}$ in a series of $16 \mu\text{s}$ simulations. From the distribution of z_T , a respective PMF profile $G_1(z_T)$ was reconstructed using the weighted histogram analysis method.⁴¹

A 2D PMF profile $G_2(z_T, u)$ with u denoting the minimal distance between the hydrophobic cores of the two bilayers excluding the lipid subjected to the umbrella potential was determined as follows. A normalized histogram $H_{z_T}(u)$ for $0.3 \text{ nm} < u < 1.9 \text{ nm}$ was calculated for each umbrella window, and the 2D PMF profile was obtained from

$$G_2(z_T, u) = -k_B T \ln H_{z_T}(u) + G_1(z_T) \quad (2)$$

Note that only z_T but not u was imposed in the simulations. That is, $H_{z_T}(u)$ was obtained from the spontaneous fluctuations in u for given z_T . A similar approach has been used previously to study cholesterol flip-flops.⁴² A derivation of this formula is given in the Supporting Information.

To estimate the free energy of the stalk (“sta”) and the splayed lipid bond (“spl”) with respect to the lamellar state (“lam”), respective partition functions

$$Z_i = \int_i dz_T du \exp[-G_2(z_T, u)/k_B T] \quad (3)$$

for $i = \text{sta, spl, lam}$ were calculated by integrating over the respective regions in the (z_T, u) plane. The free energy differences were obtained from

(41) Kumar, S.; Bouzida, D.; Swendes, R.; Kollman, P.; Rosenberg, J. *J. Comput. Chem.* **1992**, *13*, 1011–1021.

(42) Bennett, W. F. D.; MacCallum, J. L.; Hinner, M. J.; Marrink, S. J.; Tieleman, D. P. *J. Am. Chem. Soc.* **2009**, *131*, 12714–12720.

$$\Delta G_i = -k_B T \ln(Z_i/Z_{\text{lam}}) \quad (4)$$

with $i = \text{sta, spl}$. The rates for transitions from the lamellar state to a stalk or to the splayed lipid bond state, $\nu_{1,2}$, are assumed proportional to the number of lipids N in the proximal leaflets in the contact area, $\nu_{1,2} = Nr_{1,2}$. The respective normalized transition times $\tau_{1,2} = 1/\nu_{1,2}$ were estimated from the energy barrier $\Delta G^\ddagger/k_B T$ and fluctuations in the lamellar state according to

$$\frac{1}{\tau_i} = \frac{\alpha}{\tau_i^*} \exp(-\Delta G^\ddagger/k_B T); i = 1, 2 \quad (5)$$

Here, $\tau_{1,2}^*$ denote the relaxation times in the initial state which is the lamellar one here, so $\tau_1^* = \tau_2^* \equiv \tau^*$. The time τ^* was obtained from fitting the sum of two exponentials to the autocorrelation function of z_T in the lamellar state in the absence of any umbrella potential and taking the larger of the two respective relaxation times. The prefactor for transitions is expected to be proportional to $1/\tau^*$. The proportionality constant α was estimated by comparing the average waiting time τ_3 for transitions from the splayed lipid bond to the stalk intermediate observed directly with eq 5 where τ_3^* was determined in analogy to $\tau_{1,2}^*$. Note that τ_3 is independent of the number of lipids in the contact area and $\nu_3 = r_3 = 1/\tau_3$. The value for the proportionality constant obtained was $\alpha = 0.1$, and the value for the prefactor was $r_1 = \alpha/\tau_{1,2,3}^* = 5.5 \times 10^7 \text{ s}^{-1}$.

Acknowledgment. We thank T. Heimburg, R. Dimova, A. Grafmüller, and M. Kozlov for stimulating discussions.

Supporting Information Available: Simulation protocol, derivation of eq 2, comparison between minimal distance and center-of-mass distance, and complete ref.³⁷ This material is available free of charge via the Internet at <http://pubs.acs.org/>.

JA910050X